Ocean Engineering 355 (2026) 125076

Contents lists available at ScienceDirect

Ocean Engineering

journal homepage: www.elsevier.com/locate/oceaneng

Research paper

# A nested optimization framework for ship hybrid propulsion systems considering equivalent $CO_2$ emissions

Luca Maloberti, Raphael Zaccone *

*DITEN - Department of Naval Architecture, Electric, Electronic and Telecommunication Engineering, Polytechnic School, University of Genoa, Via Montallegro 1, Genoa, 16145, Italy*

ARTICLE INFO

*Keywords:*
Marine hybrid propulsion
Optimization
Energy management
Optimal design
Emission reduction
Equivalent $CO_2$

ABSTRACT

The growing demand for decarbonization of the shipping sector calls for integrated design strategies that simultaneously address energy management and propulsion system sizing. This paper presents a nested optimization framework for designing ship hybrid propulsion systems that identifies the Pareto-optimal front balancing economic and Well-to-Wake environmental performance. The framework utilizes a multi-objective genetic algorithm (NSGA-II) in the outer layer to efficiently explore the design space for battery capacity and generator sizing. For each candidate design, an inner optimization layer determines the minimum achievable greenhouse gas emissions through optimal power resource management. This nested approach ensures that each point on the resulting Pareto frontier represents a design in which both sizing and operation are simultaneously optimized. The methodological accuracy is validated by benchmarking NSGA-II against an exhaustive grid search, while its effectiveness is demonstrated in a small ferry case study by comparing results with a standard requirement-based design (RBD) approach. The results demonstrate that the optimized framework can achieve up to a 27% reduction in emissions at the same investment cost, or a 6% reduction in investment cost at the same level of emissions, compared to the RBD baseline. A sensitivity analysis is conducted to assess the method's robustness to realistic variations in power demand and to evaluate the impact of component cost fluctuations on the resulting Pareto frontier. The proposed optimization framework serves as a decision-support tool for ship designers, enabling them to make informed, consistent choices when designing marine hybrid propulsion systems. The proposed structure is generalizable to a wide range of vessel types and operational scenarios.

## 1. Introduction

### 1.1. Background and context

Atmospheric pollutant emissions are recognized as a critical global concern. As the scientific community explores alternatives to conventional solutions to safeguard long-term environmental sustainability, regulatory bodies are increasingly enforcing the adoption of sustainable practices across all sectors, with a strong emphasis on substantial and sustained reductions in greenhouse gas (*GHG*) emissions. Maritime transport, while essential for enabling large-scale global trade, also contributes significantly to environmental degradation through both air and water pollution. Currently, the shipping industry, still predominantly reliant on fossil fuels, accounts for approximately 3% of global anthropogenic *GHG* emissions, along with 13% of nitrogen oxide and 12% of sulfur oxide emissions. Moreover, it emits other harmful pollutants, including particulate matter, black carbon, and methane, all of which pose serious risks to human health and the environment. Projections suggest that, without decisive measures, emissions from the maritime sector could increase by 150% to 250% by 2050, paralleling an expected tripling of global trade volumes (Jägerbrand et al., 2019).

A wide range of adverse health effects associated with exposure to air pollution has been widely demonstrated. These include respiratory, cardiovascular, and metabolic disorders, as well as stroke, lung cancer, impaired reproductive outcomes, preterm birth, low birth weight, and increased risk of premature mortality. In 2019 alone, ambient air pollution was estimated to be responsible for approximately 4.1 million deaths globally, accounting for about 7% of all premature mortality. As such, air pollution is recognized as one of the leading risk factors in the Global Burden of Disease Study (Mueller et al., 2023).

The shipping industry is responsible for approximately 90% of global freight transport. Over the past forty years, maritime transport has experienced substantial growth, around 250%, significantly outpacing the increases in worldwide population and primary energy consumption

* Corresponding author.
*E-mail addresses:* luca.maloberti@edu.unige.it (L. Maloberti), raphael.zaccone@unige.it (R. Zaccone).

https://doi.org/10.1016/j.oceaneng.2026.125076
Received 6 July 2025; Received in revised form 5 March 2026; Accepted 12 March 2026
Available online 19 March 2026

over the same period (Bouman et al., 2017). This expansion reflects the rise in global Gross Domestic Product and highlights the pivotal role of maritime transport in facilitating international trade (Cabezas-Basurko et al., 2008). Given current trajectories, this growth trend is expected to continue, driven by ongoing globalization and rising demand for goods and connectivity. Consequently, even incremental improvements in the sector's energy efficiency, operational practices, and emission-mitigation strategies can yield substantial environmental benefits.

Maritime transport, therefore, presents a significant opportunity to take major steps toward a more sustainable future. Implementing effective policies, transitioning to cleaner fuels, and adopting innovative technologies can improve energy efficiency in the maritime sector. Coordinated action among international organizations, the shipping industry, and national governments is crucial to support this progress and ensure the sustainable development of the shipping trade.

In 2015, the Paris Agreement established ambitious targets to reduce pollutant emissions and slow global warming (UNFCCC, 2015). Therefore, decarbonizing international shipping has become a central issue for an industry that has historically relied on fossil fuels. As a consequence, adopting its initial strategy in 2018, the International Maritime Organization established concrete targets, principles, and tools for reducing greenhouse gas emissions from ships (IMO, 2018). The Energy Efficiency Existing Ship Index and the Carbon Intensity Indicator (*CII*), both of which come into effect in 2023, were recently added to the regulatory framework in addition to the *EEDI* (Tadros et al., 2023). The *CII* specifically targets operational carbon dioxide emissions by assessing how efficiently a ship transports cargo or passengers. As highlighted by Wang et al. (2021a), ensuring the robustness of *CII* metrics requires the development of refined methodologies grounded in empirical data, enabling iterative improvements and enhanced regulatory effectiveness. In this direction, Maloberti et al. (2025b) proposed an extension of the *CII* concept to encompass all GHG emissions, adopting a more holistic "Well-to-Wake" perspective that also considers emissions from battery charging for electric or hybrid vessels. Complementing these efforts, the Environmental Ship Index offers an incentive-based mechanism to evaluate and reward ships with low emissions. This index takes into account emissions in addition to $CO_2$, including nitrogen oxides ($NO_x$), sulfur oxides ($SO_x$), and shore-side electricity use, allowing port authorities to grant financial incentives to less impactful ships (Ančić et al., 2018). Despite this progress, critical challenges persist, particularly in the accuracy and consistency of emissions data, enforcement mechanisms, and the current exclusion of smaller ships from regulatory coverage. Addressing these limitations will require continuous updating of the regulatory framework, supported by advanced digital monitoring technologies, to ensure a credible and effective path to maritime decarbonization (Tadros et al., 2023).

### 1.2. Research status and challenges

Compared to other transport sectors, where standardized decarbonization strategies can often be adopted, maritime transport requires a different approach due to the substantial variation among ship types in terms of size, operational profile, and environmental conditions. Given the complexity of the sector, a one-size-fits-all solution to emissions reduction is not feasible. Technological and operational strategies must be assessed in the context of specific applications–whether deep-sea navigation, coastal operations, or inland navigation–each characterized by distinct operational requirements (Basciu et al., 2025; Jimenez et al., 2022; Lindstad et al., 2021; Maloberti et al., 2022; Inal et al., 2022). Among the most relevant solutions are alternative fuels, hybrid propulsion systems, and electrification, each offering specific advantages and constraints depending on the operational context.

Alongside advances in propulsion technology and the development of alternative fuels, operational and design optimization are crucial for achieving significant benefits in ship design and operational management. Researchers have, therefore, extensively focused on developing optimization methods for hybrid propulsion system sizing (Zaccone et al., 2021) and management, aiming to minimize environmental impact (Kanellos, 2013; Maloberti and Zaccone, 2025; Maloberti et al., 2024; Belvisi et al., 2024; Wang et al., 2024), fuel consumption (Al-Falahi et al., 2018), investment costs (D'Agostino et al., 2023), and, as well as for dynamic positioning operations (Fruzzetti et al., 2024) and route optimization (Zaccone et al., 2018).

A hybrid propulsive system introduces greater complexity, given the increased number of degrees of freedom it offers in meeting power demand during navigation. The machinery constituting the system may operate under different conditions at various parts of the overall power output, and it is not always straightforward to identify the configuration that yields maximum efficiency in a given condition. In addition, the presence of energy storage systems introduces a "memory effect", allowing energy produced at high efficiency to be stored and used later when conditions are such that the machines would be operating at lower efficiency. Power management thus benefits from model-based numerical treatment coupled with optimization algorithms. The inherent complexity of a hybrid system also makes it challenging to determine the optimal size and configuration of onboard components relative to a vessel's operational requirements.

The design of hybrid propulsion systems is currently carried out using a static, requirements-based approach (Maloberti et al., 2025a). In this industry-standard framework, power-source sizing is typically decoupled and determined by worst-case operational constraints rather than overall efficiency. Specifically, generators are sized to deliver the maximum power required by the ship, with a margin to ensure they operate at maximum efficiency. In contrast, battery energy storage systems are sized based on the energy capacity needed to meet specific mission objectives, such as zero-emission coverage or time-limited operations. Although this methodology ensures operational safety, it often results in sub-optimal propulsion configurations.

To address these inefficiencies, research has moved towards integrated design strategies. As reviewed by Cha et al. (2024), system-level optimization can be classified into sequential, iterative, simultaneous (or joint), and nested approaches. While simultaneous optimization of all variables might theoretically yield the global optimum, it requires handling a massive number of decision variables and constraints, often necessitating simplified models or computationally intensive algorithms. To manage this complexity, a nested (or bi-level) optimization framework has been adopted. This architecture effectively decouples the problem based on the distinct nature of the objectives: the outer layer addresses the strategic trade-off between investment costs and environmental impact (sizing), while the inner layer focuses exclusively on minimizing emissions for a fixed propulsion system configuration (operation). This separation ensures that each candidate design is evaluated based on its optimal operational performance, avoiding the computational burden and convergence issues typical of simultaneous optimization approaches. This approach aligns with the natural hierarchy of the problem and has been successfully demonstrated in various applications (Wang et al., 2021b; Wu and Bucknall, 2020), and validated in recent studies (Zhang et al., 2024). Similarly, recent approaches focused on battery sizing for military vessels (Belvisi and Figari, 2026) relied on exhaustive sampling of the design space to address military operating profiles.

Despite these advances, there is still a lack of a comprehensive decision-support tool specifically designed to minimize the investment cost and environmental impact of ships with hybrid propulsion systems. In particular, there remains a gap in providing a tool that optimizes these systems through a fully integrated, nested framework to guide the designer in choosing the most suitable configuration based on trade-offs, rather than relying on a static requirement-based sizing approach.

### 1.3. main contributions

To bridge this gap, this paper proposes a nested optimization framework aiming to minimize both environmental and economic impacts (Maloberti, 2025) of a hybrid marine propulsion system.

The proposed approach consists of two steps: first, the hybrid system is modeled in its entirety and integrated into an optimization algorithm that, based on the vessel's mission profile, identifies the optimal management of onboard energy resources to minimize pollutant emissions. Secondly, the optimization algorithm is integrated into an external multiobjective optimization layer that determines the optimal configuration and size of components to meet the mission profile while minimizing emissions and investment cost. More specifically, the optimization process is divided into two layers:

- The inner layer identifies the optimal power split among generators and the battery energy storage system to minimize equivalent $CO_2$ emissions.
- The outer layer optimizes the design parameters of the propulsion system, specifically, the battery capacity and the generator power, aiming to find the best trade-off between total *GHG* emissions and investment cost, adopting a Well-to-Wake assessment perspective.

This approach allows for a comprehensive assessment of hybrid propulsion configurations by decoupling the control-level problem (power resource management) from the system-level design problem. As a result, the proposed method simultaneously minimizes the total investment cost and the carbon footprint by optimizing both the onboard power split and the sizing of the propulsion system components. The framework is applied to a representative case study to demonstrate its effectiveness, and its sensitivity and robustness are evaluated through a dedicated analysis.

The main contribution of this work is the definition of a comprehensive decision-support tool that overcomes the limitations of standard requirement-based sizing by directly integrating operational performance assessment into the design loop. The proposed methodology is validated through a methodological benchmark using an exhaustive grid search to confirm the accuracy of the optimization results. Furthermore, the present study establishes a quantitative benchmark by directly comparing the optimized design to the industry-standard requirement-based sizing approach. The operational performance of the baseline configuration is assessed using the proposed inner-layer energy management, which minimizes emissions while satisfying physical and operational constraints. The framework provides robust decision support by generating a Pareto frontier of optimal solutions that balance investment costs with Well-to-Wake GHG emissions. The computational convergence and the stability of the results are assessed through sensitivity analyses on algorithm parameters (population size and number of generations), as well as on power demand and system component specific costs. This ensures that the identified trade-off trends remain consistent across varying operational, economic, and numerical settings.

The remaining of the paper is organized as follows: Section 2 describes the proposed methodology, including the system modeling approach, the nested structure of the optimization problems, and their integration; Section 3 describes the case study; Section 4 presents the results obtained and the methodological benchmark; Section 5 provides a sensitivity analysis to assess the framework's sensitivity to variation in input parameters; and finally, Section 6 draws conclusions and identifies limitations of the study.

## 2. Methodology

### 2.1. Propulsion system modeling

The modeling approach adopted in this study aims at maintaining a consistent level of approximation across all system components. Static lumped-parameter models are used to estimate key performance indicators and facilitate a comparative assessment of different propulsion configurations. The primary objective of the modeling effort is to quantify how operational decisions, such as the power split among onboard energy sources, and design choices, such as the sizing of propulsion system components, affect overall system performance across one or more mission profiles. This section presents the mathematical models adopted for the key components of the propulsion system, namely the generators, the battery energy storage system, and the associated electrical subsystems. A schematic representation of the hybrid propulsion architecture is shown in Fig. 1.

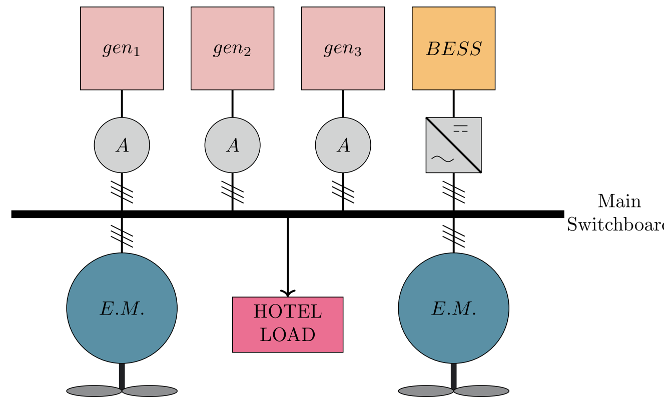


**Fig. 1.** Schematic representation of the hybrid propulsion system.

The diesel generators are modeled using Specific Fuel Oil Consumption (*SFOC*) to estimate the fuel mass flow rate as a function of the delivered power (Ashok et al., 2018):

$$\dot{m}_{fuel} = P_B \, SFOC \tag{1}$$

In principle, the Specific Fuel Oil Consumption depends on both the engine's power output and its speed. However, because diesel generator speed is typically controlled, the explicit dependence on speed can be omitted. Consequently, *SFOC* is represented as a second-order polynomial function of engine power (Ghimire et al., 2021):

$$SFOC = a\left(\frac{P_B}{P_{MCR}}\right)^2 + b\frac{P_B}{P_{MCR}} + c \tag{2}$$

Where $P_{MCR}$ the rated power of the generators, and $a$, $b$, and $c$ are the polynomial coefficients estimated to fit manufacturer data. The adopted values, reported in Table 1, are based on data from representative generators of similar capacity (Isotta Fraschini Motori, 2026). Similar-sized engines are assumed to have the same specific consumption pattern and values. Fig. 2 illustrates the *SFOC* curve, considering Marine Diesel Oil (*MDO*) as fuel. It is worth noting that the minimum specific consumption range for the considered diesel engine stands between 70 and 90 per cent of its nominal power.

This model assumes a linear relationship between the emitted pollutant and fuel consumption, represented by the emission factor, which is the amount of pollutant emitted per unit of fuel burned.

The battery state-of-charge (*SoC*) is expressed as:

$$SoC(t) = \frac{Q_0 - \int_0^t i(\tau)d\tau}{Q_{max}} \tag{3}$$

Where $Q_0$ is the charge at time $t = 0$. For technological reasons, the state-of-charge (*SoC*) is typically maintained within 30% and 85%. The battery efficiency $\eta_{BESS}$ is defined as the ratio between the battery energy output $E_{discharge}$ and input $E_{charge}$, and represents the energy lossess $E_{loss}$ due to the inner resistance of the battery:

$$\eta_{BESS} = \frac{E_{discharge}}{E_{charge}} = \frac{E_{charge} - E_{loss}}{E_{charge}} \tag{4}$$

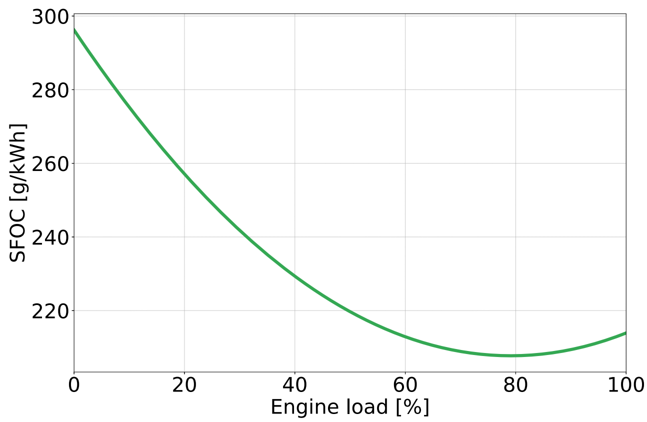


**Fig. 2.** Specific fuel oil consumption curve.

**Table 1**
Efficiency of the key electrical components and *SFOC* coefficient values.

| Component | Efficiency |
|---|---|
| $\eta_{EPM} - \eta_{alt}$ | 0.96 |
| $\eta_{DC/AC} - \eta_{AC/DC}$ | 0.99 |
| $\eta_{DC/DC} - \eta_{AC/AC}$ | 0.97 |
| $\eta_{BESS}$ | 0.95 |
| *SFOC* coefficient | Value |
| a | 0.014 |
| b | −2.24 |
| c | 296.20 |

In this model, $\eta_{BESS}$ represents the combined charge-discharge efficiency. Since the optimization evaluates complete operational cycles, this lumped parameter accurately captures total energy losses, avoiding the computational complexity of an asymmetric efficiency model.

The *SoC* expression can then be rearranged by expressing Eq. (3) in terms of energy and considering the battery efficiency defined in Eq. (4), obtaining to the following formulation:

$$\begin{cases} SoC(t) = SoC(0) - \dfrac{\beta}{E_{BESS}} \displaystyle\int_0^T P_{BESS}(t)dt \\ \beta = \begin{cases} 1 & \text{if } P_{BESS} \le 0 \\ \eta_{BESS} & \text{if } P_{BESS} > 0 \end{cases} \end{cases} \quad (5)$$

Where $SoC(0)$ is the initial State-of-Charge of the battery, $P_{BESS}$ is the power delivered or absorbed by the *BESS*, and $E_{BESS}$ is the nominal battery energy.

To obtain realistic performance estimation for the power system, the efficiency of key electrical components may be assumed, including electric motors, alternators, battery system, and various types of converters. The assumed efficiency values for the electrical components are summarized in Table 1.

### 2.2. Inner optimization layer

The inner layer of the proposed nested optimization framework features a power management strategy optimization, proposed by the authors in Maloberti and Zaccone (2025), aiming to find the optimal power split among the power system components to minimize the equivalent $CO_2$ emissions produced by the ship during its mission. Fig. 3 provides a qualitative example of an input load profile. The mission is discretized over time-instants $t_j$, $j = 0 \dots T$ corresponding to the variations of the required power. Every step represents a shift in the power demand $P_j$ that the system has to meet at each discrete time instant.

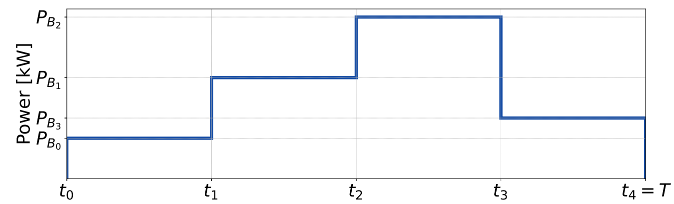


**Fig. 3.** Example of a load profile.

The minimum of the objective function obtained in this layer became one of the objective functions of the outer layer, contributing to finding the best trade-off described in Section 2.3. Parametrization, constraints, and objective function are summarized hereinafter.

#### 2.2.1. Parametrization

The optimization variables are the load coefficients $\alpha$ of the diesel generators, which define the power output as a fraction of their maximum power. At time $t_j$, the optimization variables can be stored into a vector $X_j$:

$$X_j = \left\{ \alpha^j_{DG_1}, \alpha^j_{DG_2}, \dots \alpha^j_{DG_n} \right\} \quad (6)$$

Where $\alpha^j_{DG_i}$ are the load coefficients of the $i^{th}$ Diesel Generator (*DG*) at time $t_j$, and $n$ is the number of *DG* installed on-board. A candidate solution is structured as follows:

$$\mathbf{X} = \left\{ X_j \right\}, \ j = 0 \dots (T-1) \quad (7)$$

The power delivered by the $i^{th}$ generator at each time-instant $t_j$ is derived through to the following equation:

$$P^j_{DG} = \alpha^j_{DG_i} P^{max}_{DG_i} \quad (8)$$

The battery power for each time-instant is derived by subtracting the power delivered by the generators from the total power required.

#### 2.2.2. Objective function

Since the primary goal is to mitigate the impact of global warming, the inner optimization problem minimizes Well-to-Wake greenhouse gas emissions, expressed through equivalent $CO_2$, throughout the entire mission:

$$CO_{2\,eq} = EF_{fuel} \sum_{j=0}^{T} \sum_{i=1}^{n} \alpha^j_{DG_i} P^{max}_{DG_i} SFOC_i(\alpha^j_{DG_i}) \Delta t_j \quad (9)$$

It is worth noting that the shore power network is not used, as the BESS is charged exclusively by the on-board generators, and no cold ironing operations are carried out. Therefore, the only GHG emissions are those resulting from the use of the generators. Where $EF_{fuel}$ is the equivalent $CO_2$ emission factor for the *MDO*, $\alpha^j_{DG_i}$ is the load coefficient of the $i^{th}$ *DG* at time $j^{th}$, $P^{max}_{DG_i}$ is its maximum power, and $SFOC_{i,j}$ is the specific fuel oil consumption of the $i^{th}$ *DG* at the $j^{th}$ time.

The equivalent $CO_2$ emissions aggregate the impact of all greenhouse gases emitted during fuel combustion, e.g., carbon dioxide ($CO_2$), methane ($CH_4$), and nitrous oxide ($N_2O$). Each gas contributes differently to global warming, as quantified by its Global Warming Potential (*GWP*), which expresses its impact relative to that of $CO_2$ over 100 years. Table 1 presents the *GWP* of the primary *GHG* emitted during the fuel combustion process and the emission factor of the equivalent $CO_2$, obtained through the following equation:

$$EF_{CO_{2\,eq}} = \sum_i GWP_i \, EF_i \quad (10)$$

Where $i$ represent the $i^{th}$ *GHG*. *GHG* emissions, calculated through $CO_{2\,eq}$, are proportional to fuel consumption, where the proportionality factor is the emission factor calculated by Eq. (10).

#### 2.2.3. Constraints

The power generated by each generator must be within the allowable limits. To ensure this operational constraint, the load coefficients of the generators must be kept between 0 and 1, as indicated in the following equation:

$$0 \leq \alpha^{j}_{DG_i} \leq 1 \tag{11}$$

The power delivered or absorbed by the *BESS*, obtained by subtracting the generator power from the power required by the load, is constrained between the maximum power input and the maximum power output that the battery system can tolerate. Therefore, the power balance constraint can be written as follows:

$$-P^{max,c}_{BESS} \leq \sum_{i=1}^{n} P_{i,j} - P_{load_j} \leq P^{max,d}_{BESS} \tag{12}$$

Where $P_i$ is the power output of the $i^{th}$ generator, $P_{BESS}$ is the *BESS* power, $P_{load}$ is the power demand, and $P^{max,d}_{BESS}$, $P^{max,c}_{BESS}$ are the maximum power in discharge and charge, respectively.

Moreover, two constraints for the Battery Storage System need to be set. The *SoC* of the battery system is bounded between a minimum and maximum value to maximize its durability over time:

$$SoC^{min} \leq SoC_j \leq SoC^{max} \tag{13}$$

The $SoC_j$ at time $t_j$ obtained by discretizing Eq. (5), is given by:

$$SoC_j = \frac{1}{E_{max}}\left(E_0 - \beta \sum_{p=0}^{j} P_{BESS_p} \Delta t_p\right) \tag{14}$$

Where $\Delta t_p = t_p - t_{p-1}$. Furthermore, the battery soc needs to be the same at the beginning and end of the mission to keep the results consistent:

$$SoC_0 = SoC_T \tag{15}$$

A zero-emission operating constraint is introduced to require generators to shut down at specific time-instants $t_j$, corresponding to operations in emission-sensitive areas, such as ports or protected areas. During these intervals, the required power must be provided by the *BESS*. The constraint is formulated as follows:

$$P^{k}_{gen_i} = 0 \tag{16}$$

Where $k$ denotes the specific time-instant in which zero-emission mode is activated.

### 2.3. Outer optimization layer

The outer layer of the nested optimization aims to find the optimal size of the components to minimize both the Well-to-Wake $GHG$ emissions produced by the vessel over the mission and the hybrid propulsion system cost, using a Pareto optimization approach. Parametrization, constraints, and objective functions are defined and analyzed in the following subsections.

#### 2.3.1. Parametrization

The outer optimization layer relies on two key design variables for the hybrid propulsion system: the battery energy storage capacity $E_{BESS}$, representing the total battery capacity, and the maximum generator power $P^{max}_{gen}$, defining the peak power output of the diesel generators. These variables together define the candidate system configuration:

$$\mathbf{Z} = \left\{ E_{BESS}, P^{max}_{gen} \right\} \tag{17}$$

This flexibility enables the generation of configurations tailored to specific mission profiles. By adjusting $E_{BESS}$ and $P^{max}_{gen}$, the optimization process can determine system configurations that enhance both environmental and economic performance. The two parameters define the physical boundaries of the system and serve as the basis for subsequent analyses and optimization phases.

#### 2.3.2. Objective functions

The optimization framework is developed to minimize both the carbon footprint of the ship and the cost of the propulsion system. The carbon footprint is measured in terms of total greenhouse gas emissions, expressed in terms of the Well-to-Wake equivalent $CO_2$ mass. This value, which depends on the specific propulsion configuration, is minimized within the inner level of the optimization process and is defined in the following expression:

$$f_1(\mathbf{Z}) = CO^{min}_{2\,eq}(\mathbf{Z}) \tag{18}$$

This formulation enables a comprehensive assessment of environmental performance by including all relevant sources of emissions. The economic objective function, denoted as $C_{sys}$, represents the combined cost of the generators and the battery energy storage system, and is determined using the following equation:

$$C_{sys} = sc_{gen}\, P^{gen}_{B}\, N_{gen} + sc_{BESS}\, E_{BESS} \tag{19}$$

Where $sc_{gen}$ and $sc_{BESS}$ are, respectively, the specific costs of the generators, assumed in $450\,€/kW$ and the specific cost of the *BESS*, assumed to be $200\,€/kWh$, and $N_{gen}$ denotes the number of generators onboard.

Therefore, the second objective function can be expressed as:

$$f_2(\mathbf{Z}) = C_{sys}(\mathbf{Z}) \tag{20}$$

These two objectives capture the trade-off between cost and environmental impact, forming the basis for Pareto optimal solutions. The exploration of propulsive configurations produces the Pareto frontier of the Pareto-optimal solutions. Depending on the weight assigned to the two objective functions, it is possible to select from the Pareto-optimal set the configuration that best meets the specific design requirements of the case study.

#### 2.3.3. Constraints

To guarantee that the solutions obtained are both realistic and technically feasible, the optimization process includes constraints that limit the allowable values of battery capacity $E_{BESS}$ and maximum generator power $P^{max}_{gen}$:

$$\begin{cases} E_{BESS,\,lower} \leq E_{BESS} \leq E_{BESS,\,upper} \\ P^{max}_{gen,\,lower} \leq P^{max}_{gen} \leq P^{max}_{gen,\,upper} \end{cases} \tag{21}$$

The terms $P^{max}_{gen,lower}$ and $P^{max}_{gen,upper}$ define the lower and upper bounds for the maximum generator power, while $E_{BESS,lower}$ and $E_{BESS,upper}$ specify the admissible range for the battery energy capacity. A minimum value of zero for $E_{BESS}$ corresponds to a configuration with only generators installed on board. These constraints are essential to ensure the physical feasibility of the propulsion configuration, keeping the results within realistic technological and operational limits.

### 2.4. Nested optimization problem formulation

The problem can be formulated as a two-layer multi-objective optimization problem. The aim is to minimize two conflicting cost functions, greenhouse gas emissions and propulsion system investment cost, while satisfying the defined constraints. By integrating the design variables (Eq. (17)), objective functions (Eq. (18), (20)), and constraints (Eq. (21)), the complete optimization problem can be defined as follows:

$$\begin{cases} \min\limits_{\mathbf{Z}} \left\{ CO^{min}_{2\,eq}(\mathbf{Z}),\, C_{sys}(\mathbf{Z}) \right\} \\ s.\ t.: \\ E^{min}_{BESS} \leq E_{BESS} \leq E^{max}_{BESS} \\ P^{min}_{gen} \leq P_{gen} \leq P^{max}_{gen} \end{cases} \tag{22}$$

Where the first objective function $CO^{min}_{2\,eq}$ is obtained through the power-split optimization performed in the inner layer.

**Table 2**
Main characteristics of the case-study vessel.

| | |
|---|---|
| Length | 28.73 $m$ |
| Breadth | 7.02 $m$ |
| Depth | 2.6 $m$ |
| Draft | 1.22 $m$ |
| Displacement | 120 $t$ |
| Cruise speed | 18 $kn$ |
| Low Speed | 13 $kn$ |
| Passenger | 516 |

By combining Eqs. (9), (11)–(13), (15), the inner layer optimization formulation is the following:

$$\begin{cases} \min\limits_{\mathbf{X}} \; CO_{2\,eq}(\mathbf{X}) \\ s.\ t.: \\ 0 \leq \alpha^j_{gen_i} P^{max}_i \leq P^{max}_i \\ -P^{max,c}_{BESS} \leq \sum_{i=1}^{n} P_{i,j} - P_{load_j} \leq P^{max,d}_{BESS} \\ SoC^{min} \leq SoC_j \leq SoC^{max} \\ SoC_0 = SoC_T \\ m_X \leq X_{on-board} \\ m_{pilot} \leq pilot_{on-board} \\ P^k_{gen_i} = 0 \\ (\alpha^j_{DG_i} P^{max}_i = 0) \vee (0.2 \leq \alpha^j_{DG_i} P^{max}_i \leq 0.95\ P^{max}_i) \end{cases} \tag{23}$$

## 3. Case study

### 3.1. Case-study vessel

The case-study vessel, whose main characteristics are reported in Table 2, is a small ferry “Cinque Terre” Marine Protected Area in Italy. The ferry can carry up to 516 passengers when fully loaded. Its high transport capacity relative to its size makes it an efficient solution for high-density routes in areas with restricted maneuvering areas.

Fig. 1 provides a schematic representation of the hybrid propulsion system, which combines generators and a battery energy storage system. These components meet the propulsion and the hotel power requirements. The battery pack enables zero-emission mode navigation, particularly during low-speed operations in ports and marine protected areas, while also allowing the generators to operate near their optimum efficiency at each time instant, thus reducing their consumption and the pollutant emissions. Azimuthal thrusters provide excellent maneuverability, which is crucial for navigation in narrow areas. The propulsive power as a function of the vessel speed is shown in Fig. 4. The hotel load is assumed to be 50 $kW$ with no dependence on speed.

### 3.2. Mission profile

The ferry under study operates within the “Cinque Terre” Marine Protected Area, an area subject to strict environmental regulations. The mission takes place between La Spezia and Levanto, with intermediate stops at the ports of Portovenere, Riomaggiore, Manarola, Vernazza, and Monterosso, as illustrated in Fig. 5. From the port of La Spezia, the ferry sails at 18 knots to Portovenere, where it makes a brief 20-min stop to allow passengers to embark and disembark. The ferry then resumes cruising until it enters the protected area, where the speed is reduced to 13 knots, in compliance with regulatory limits imposed within the protected area. Upon exiting the MPA, the ship resumes a speed of 18 knots for the last leg to Levanto. The stop at the port of Levanto lasts 80 min, after which the vessel takes the backward route to La Spezia. Table 3 reports the code used in the figures to identify the ports visited by the vessel along its mission route. Fig. 6 presents a graph of the power profile during the mission. The green and red vertical lines indicate the entry into and exit from the marine protected area, respectively.

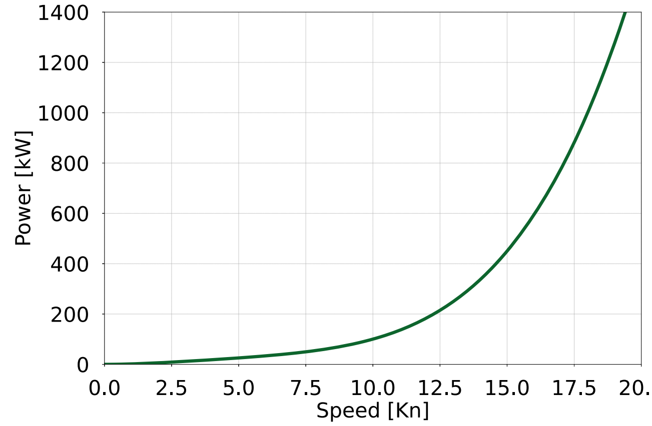


**Fig. 4.** Propulsive power curve in function of ship’s speed.

**Table 3**
Nomenclature of the ports visited during the mission .

| Name | Port |
|---|---|
| Port A | La Spezia |
| Port B | Portovenere |
| Port C | Riomaggiore |
| Port D | Manarola |
| Port E | Vernazza |
| Port F | Monterosso |
| Port G | Levanto |

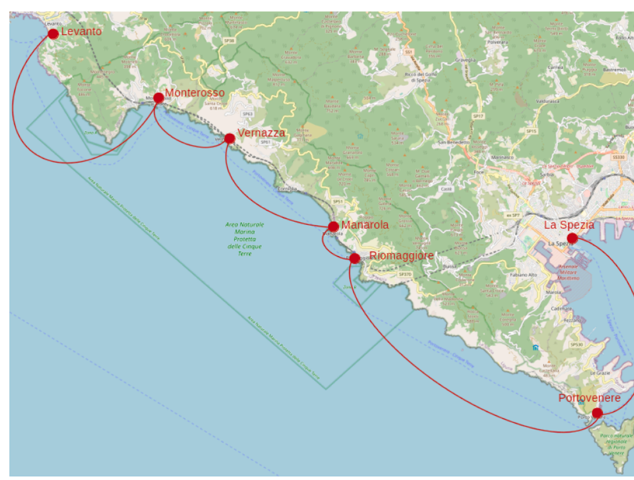


**Fig. 5.** The “Cinque Terre” Marine Protected Area.

### 3.3. Reference design

Traditionally, propulsion system sizing relies on a static, requirement-based approach, in which components are dimensioned primarily to meet operational constraints. To assess the effectiveness of the proposed optimization framework, a reference baseline configuration has been identified. This configuration is sized according to the standard design approach based on the following principles:

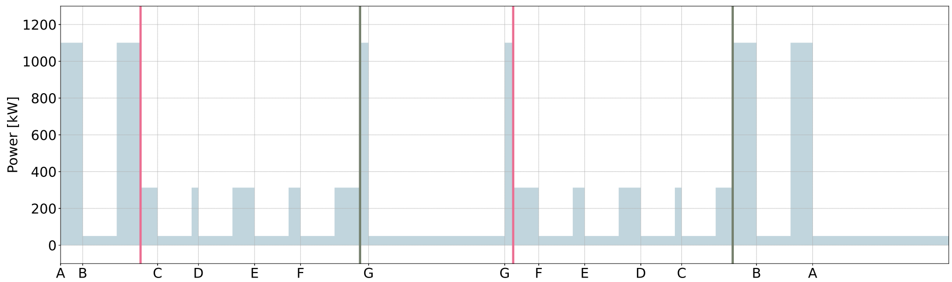


**Fig. 6.** Required power profile over the mission.

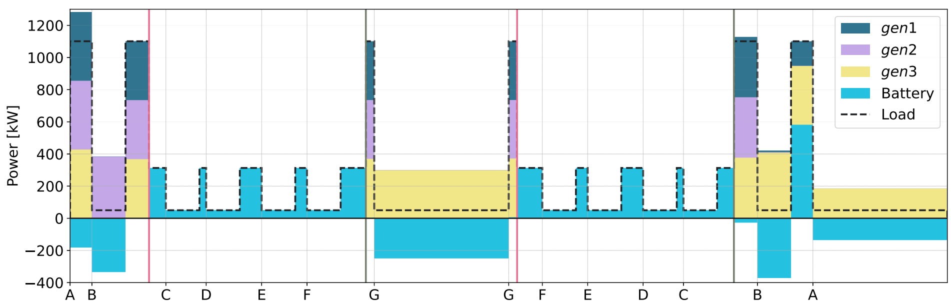


(a) Power split

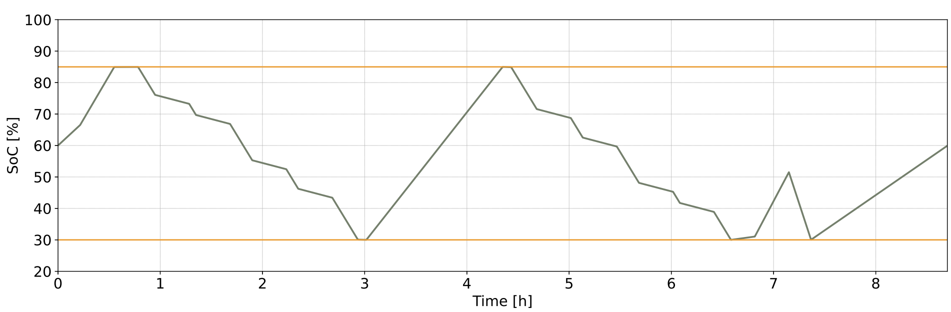


(b) State-of-Charge

**Fig. 7.** Baseline configuration.

- The Diesel Generators are sized to meet the maximum power load required by the mission profile with all three generators active and operating at 85% of their rated power, i.e., the maximum-efficiency condition (minimum SFOC). This leads to three units rated at 430 $kW$ each.
- The Battery Energy Storage System is sized according to a range requirement, i.e., to carry enough energy to allow the vessel to cross the protected zone without engaging the diesel generators (zero-emission mode, see Section 2). This leads to a capacity of 587 $kWh$.

The optimal operational performance of the baseline configuration can be achieved by applying inner-layer energy management optimization, as illustrated in Fig. 7. Specifically, Fig. 7(a) depicts the optimal power split among energy sources, while Fig. 7(b) shows the evolution of the battery state-of-charge throughout the mission. The adopted reference baseline results in 1194.7 $t/y$ of equivalent $CO_2$ emissions, with an investment cost of 697.9 $k€$.

### 3.4. Materials

The optimization framework proposed in this paper was implemented in `Python`, employing state-of-the-art numerical optimization libraries. In particular, `scipy.optimize.minimize` was used for the inner layer. Meanwhile, `pymoo` was adopted to implement the Non-Dominated Sorting Genetic Algorithm II (NSGA-II) for multi-objective optimization performed in the outer layer. The use of this programming language ensures complete reliance on free and open-source software, providing greater accessibility, transparency, and adaptability of the tool for future research and industrial applications. It is essential to note, however, that the presented optimization framework implementation is solver-agnostic and can be replicated employing various programming languages and optimization environments. Simulations were carried out on an Asus ROG G14 with AMD Ryzen 9-6900HS 4.9 GHz CPU, 16 GB RAM, running Fedora 42 OS.

## 4. Results

This section presents the application of the proposed methodology to the case study ferry. The outcomes of the optimization framework described in Sections 2.2 to 2.4 are presented and compared with the baseline, highlighting the specific advantages of the proposed approach. The design variables $E_{BESS}$ and $P_{gen}^{max}$ are bound within the intervals [0 $kWh$, 1000 $kWh$] and [400 $kW$, 600 $kW$], respectively.

Fig. 8 shows the results obtained considering a population of 75 individuals evolving over 10 generations, color-mapped on the *GHG*

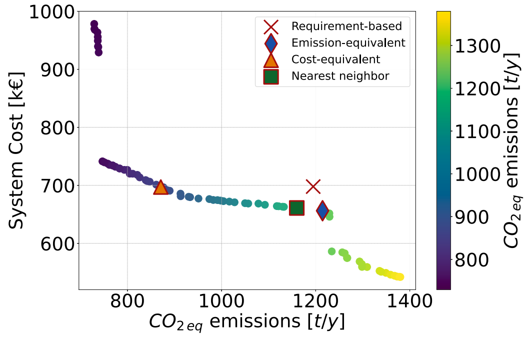


(a) Best Pareto frontier

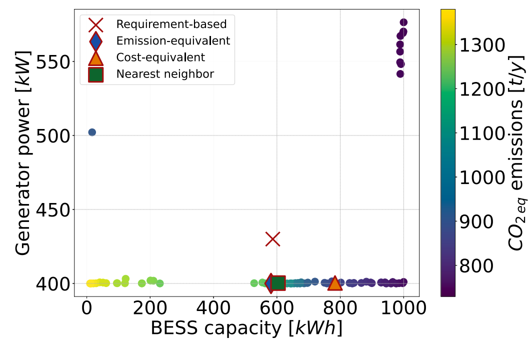


(b) System sizing solutions

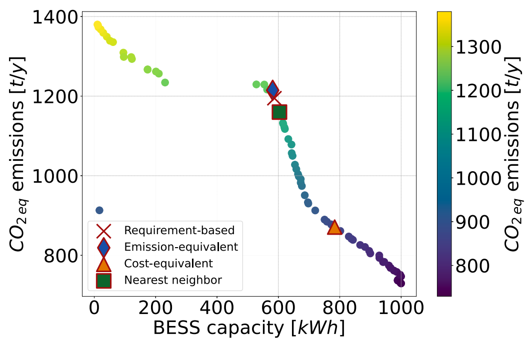


(c) $CO_{2\,eq}$ emissions as a function of the *BESS* capacity

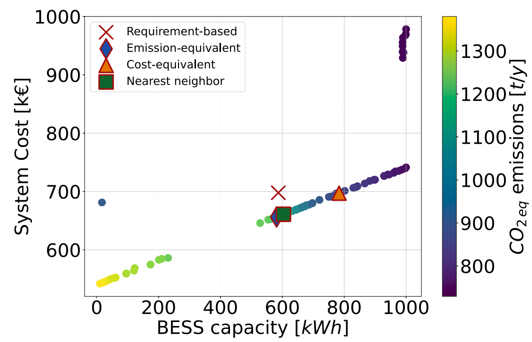


(d) Systemn investment cost as a function of the *BESS* capacity

**Fig. 8.** Results color-mapped on *GHG* emissions.

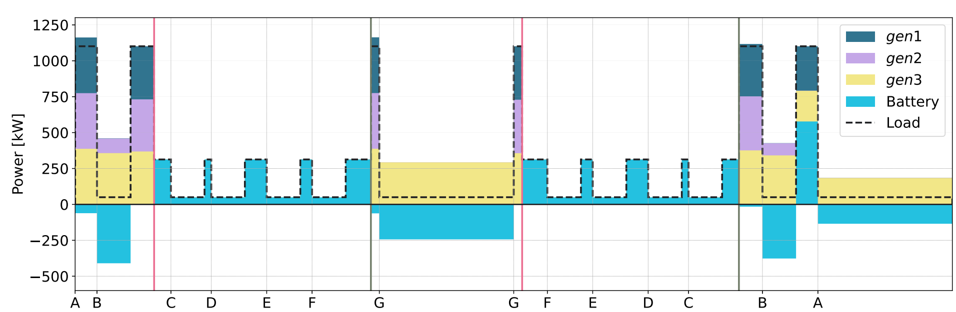


(a) Power split

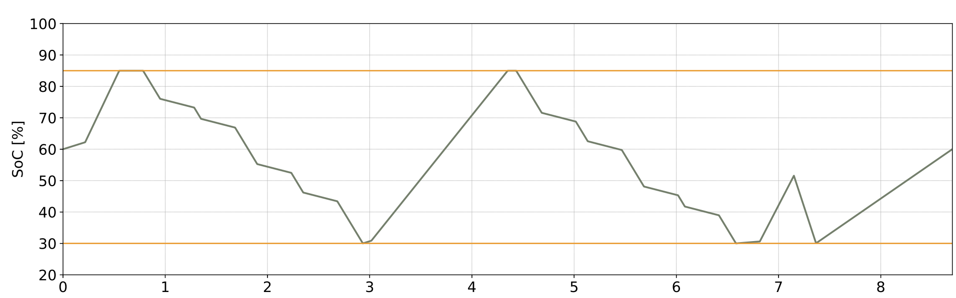


(b) State-of-Charge

**Fig. 9.** Emission-equivalent configuration, featuring 581 *kWh BESS*, and $3 \times 400$ *kW* generators.

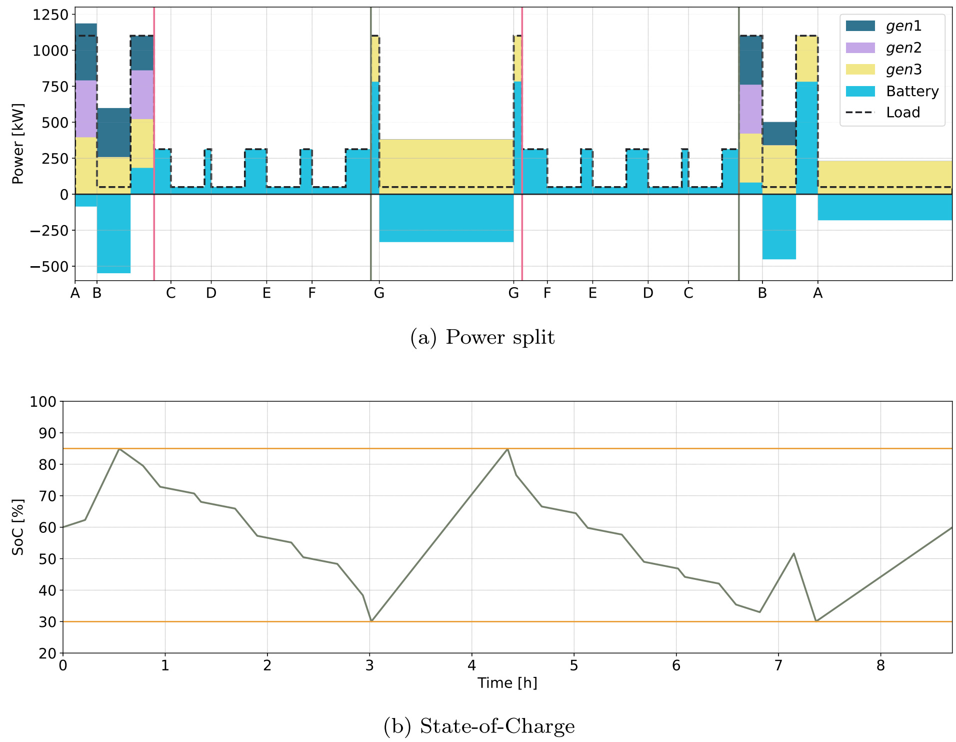


**Fig. 10.** Cost-equivalent configuration, featuring 783.5 *kWh BESS*, and $3 \times 400$ *kW* generators.

emissions. The red cross in the graphs represents the results obtained from manual requirement-based sizing described in Section 3.3. As shown in Fig. 8(a), the point obtained by this procedure is a dominated solution, so it is not part of the Pareto frontier. In particular, for the same investment cost, the optimized framework identifies a solution that reduces emissions by 27%. Conversely, maintaining the same annual emissions, it finds a configuration that is 6% cheaper. Furthermore, the nearest-neighbor solution on the Pareto frontier offers a simultaneous reduction of 3% in emissions and 5% in costs. This shows how a static, requirement-based sizing procedure can yield suboptimal component sizing, even when the power management strategy is optimized. By adopting the proposed optimized procedure, small variations in the propulsion system configuration lead to significant improvements in emissions and costs, thereby identifying better trade-offs between the two objectives.

As shown in Fig. 8(a), the lowest emissions are achieved at a system implementation cost of almost 1 million euros. However, costs can be reduced by more than 20% with a slight increase in pollutant emissions. As shown in Fig. 8(b), this significant cost decrease is achieved by reducing the output of the three generators to 400 $kW$ each. The other points on the Pareto frontier are also obtained by considering 400 kW generators, highlighting that installing larger generators offers no significant benefit in either economic or environmental terms. Fig. 8(c) shows the *GHG* emissions as a function of the *BESS* capacity. The cost trend as a function of battery capacity, presented in Fig. 8(d), shows that increasing battery capacity reduces annual emissions but also leads to a linear increase in costs. None of the solutions on the Pareto frontier corresponds to an available battery pack energy between 250 and 500 $kWh$. This suggests that installing capacities in this range is not beneficial from either a cost or an emissions perspective. Figs. 9–11 illustrate the power split and battery state-of-charge for the emission-equivalent, cost-equivalent, and nearest-neighbor configurations, respectively.

### 4.1. *Methodological benchmark: NSGA-II vs. Exhaustive grid search*

The effectiveness and methodological superiority of the proposed nested optimization framework are demonstrated by benchmarking the NSGA-II approach against an exhaustive grid search evaluation. Although the primary objective of this study is to develop a decision-support tool rather than to compare heuristic algorithms, validation of the selected method through exhaustive grid search evaluation over a discretised design space establishes a robust quantitative baseline for the accuracy of the proposed framework. It should be noted that, in this scenario, the power split distribution is optimized for each configuration using the same internal layer as employed in the main proposed framework. The exhaustive approach necessitates defining a discrete space of decision variables, resulting in the evaluation of a finite set of predetermined configurations. In this benchmark, generator power was discretized to 400, 450, 500, 550, and 600 $kW$, while battery capacity ranged from 0 (configuration without battery) to 1 $MWh$ with a step of 25 $kWh$.

Fig. 12 presents a scatter plot of the results obtained for all configurations evaluated with this approach, comparing the two objectives. This comparison demonstrates the advantages of the proposed nested NSGA-II framework. In particular, the NSGA-II evolutionary algorithm approach performed better than the brute-force approach, efficiently identifying superior configurations by thoroughly exploring the design space.

## 5. Sensitivity analysis

This section aims to assess the robustness of the proposed methodology to variations in algorithm parameters and input. The first key aspect of this analysis is the impact of population size and number of generations on the convergence and quality of the Pareto frontier.

Fig. 13 presents the Pareto frontiers obtained with different combinations of population sizes (from 25 to 100 individuals) and

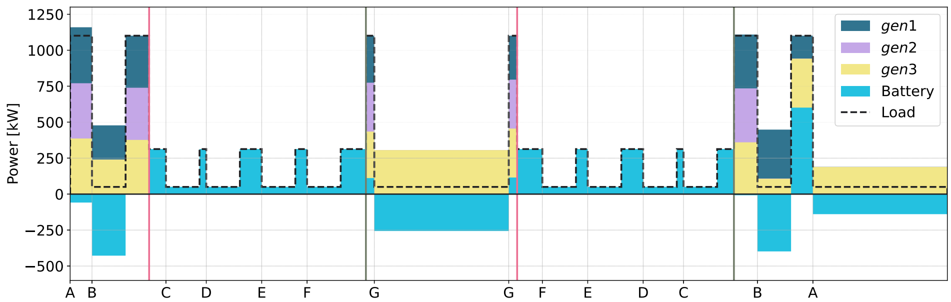


(a) Power split

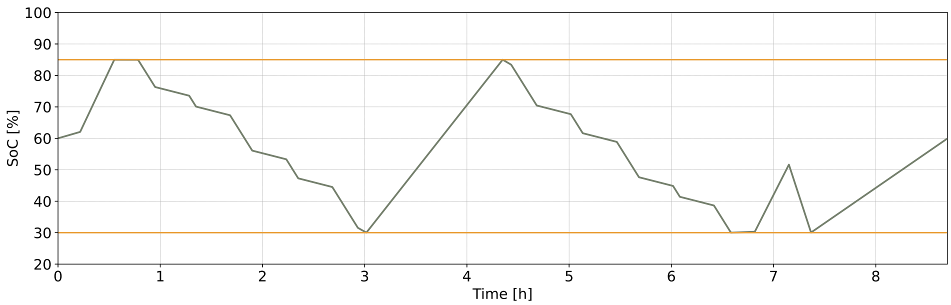


(b) State-of-Charge

**Fig. 11.** Nearest-neighbor configuration, featuring 603.5 $kWh$ $BESS$, and $3 \times 400$ $kW$ generators.

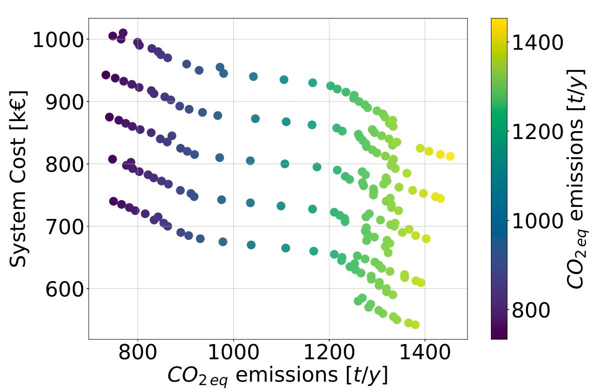


**Fig. 12.** Exhaustive grid search evaluation system-sizing optimization results.

numbers of generations (from 5 to 15). The stability of the Pareto frontier confirms the convergence behavior of the NSGA-II algorithm under changes in population size and the number of generations. Indeed, increasing these parameters results in a progressively denser frontier while the overall shape remains stable, indicating that the algorithm reliably converges to the Pareto-optimal set. Furthermore, the influence of the ship's power demand profile on the Pareto front has been assessed to evaluate the stability of the optimization results under fluctuations in load requirements. Specifically, variations of ±5% and ±15% with respect to the original power profile have been applied. These perturbations aim to simulate potential deviations due to design uncertainties, sea state, operational variability, e.g., displacement and aging, or modeling assumptions.

Fig. 14 illustrates how the optimal solutions vary in response to changes in the load power demand. As expected, a reduction in the required power leads to lower greenhouse gas emissions along the Pareto frontier, while an increase in power demand results in higher emissions. Fig. 15 shows the combinations of design variables that generate the solutions populating the Pareto frontier. The observations made for the original load profile remain valid even when the ship's power requirements are perturbed. Overall, the results confirm the robustness of the proposed optimization methodology. The solutions remain largely consistent across all scenarios, indicating a limited sensitivity to the installed generator capacity. Instead, the battery capacity remains the most influential design variable for both investment cost and emissions objectives.

To further evaluate the practicality and robustness of the proposed method, an additional sensitivity analysis was performed on key economic parameters, specifically the specific investment costs of the battery energy storage system ($sc_{BESS}$) and the diesel generators ($sc_{gen}$). As shown in Fig. 16, these costs were varied by ±50% from their baseline values to simulate substantial market price fluctuations and assess their impact on the Pareto frontier. Although these cost variations result in a vertical shift of the Pareto frontier, reflecting changes in total investment cost, the geometric shape of the frontier and the distribution of optimal solutions remain consistent. It is important to underline that the fundamental design strategy is preserved: the optimization framework consistently identifies configurations with the smallest feasible generator sizes as most advantageous, consistent with the baseline scenario. This consistency across both operational and economic perturbations suggests, with reasonable confidence, that the proposed methodology performs reliably for the case study considered in this analysis. Moreover, the optimization framework's general structure suggests the tool can be effectively adapted to various vessel types and mission profiles.

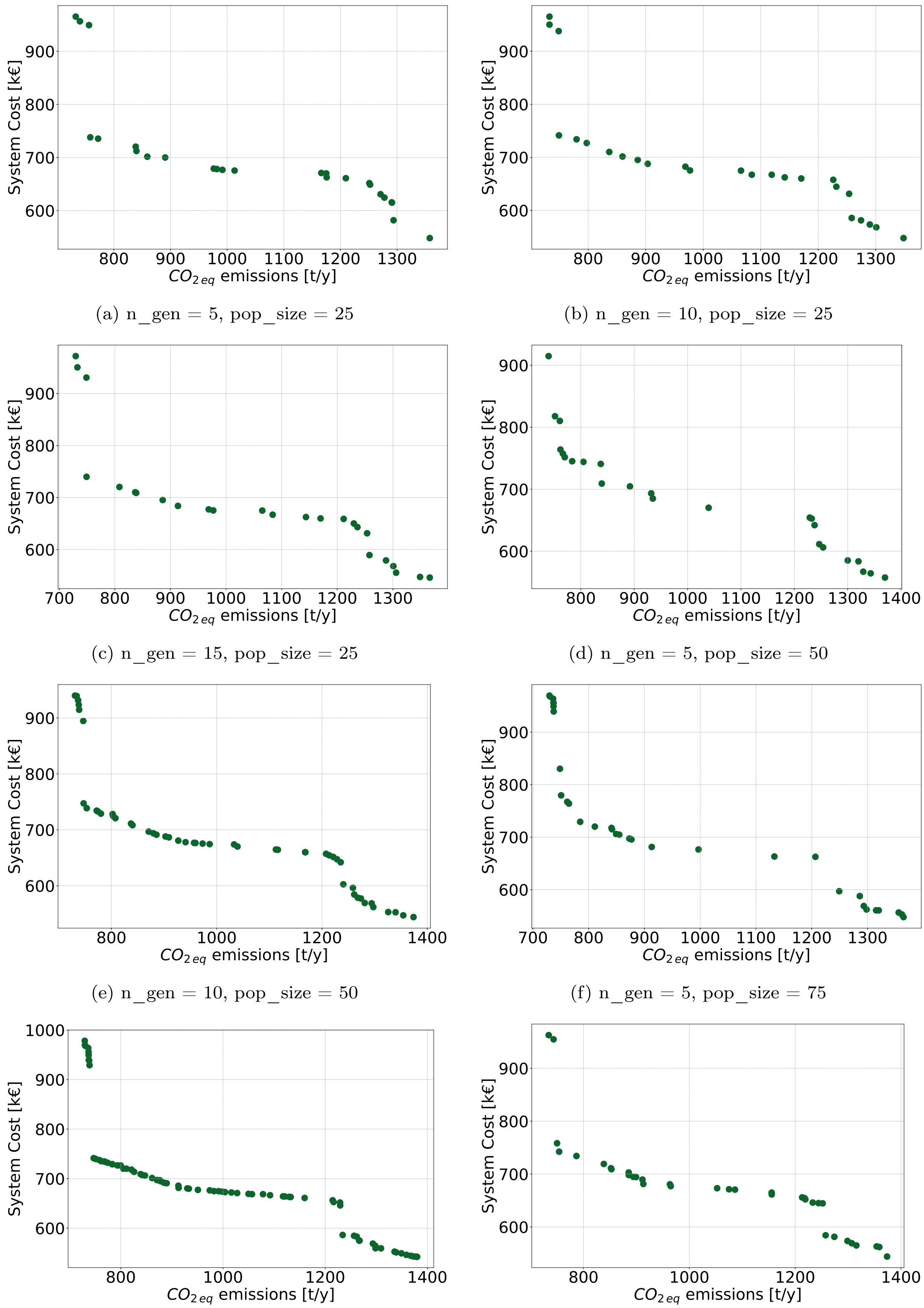


(a) n_gen = 5, pop_size = 25

(b) n_gen = 10, pop_size = 25

(c) n_gen = 15, pop_size = 25

(d) n_gen = 5, pop_size = 50

(e) n_gen = 10, pop_size = 50

(f) n_gen = 5, pop_size = 75

(g) n_gen = 10, pop_size = 75

(h) n_gen = 5, pop_size = 100

**Fig. 13.** Pereto frontier convergence analysis varying population size and number of generations.

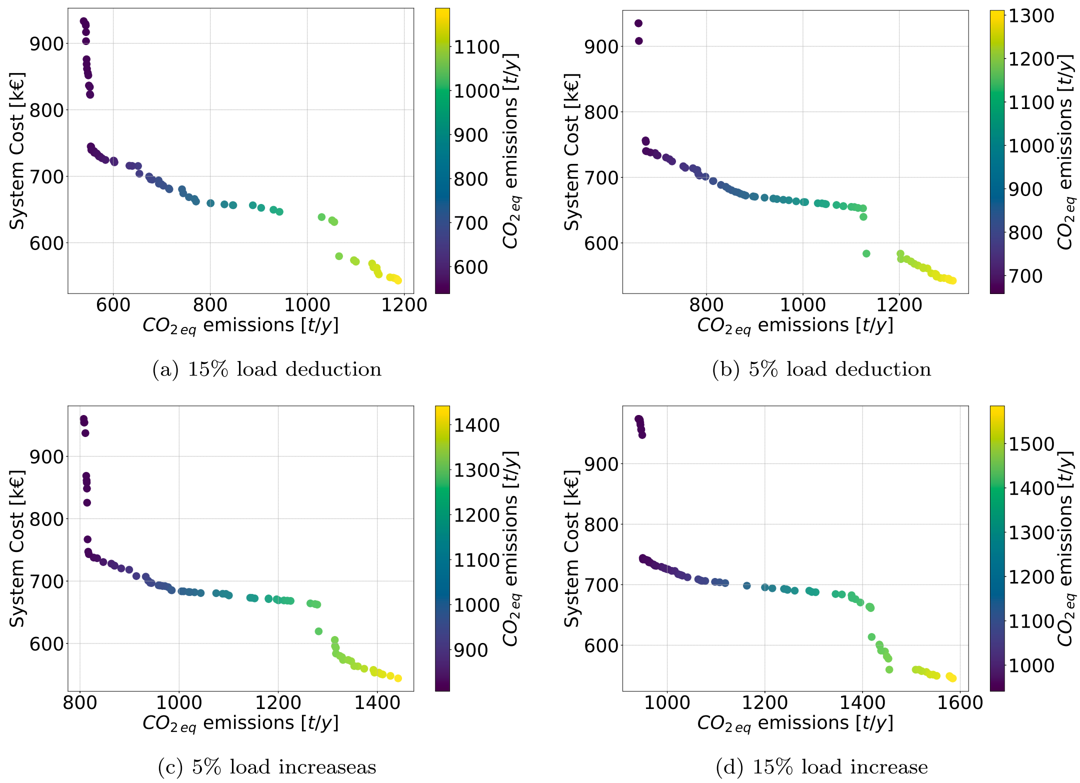


(a) 15% load deduction
(b) 5% load deduction
(c) 5% load increaseas
(d) 15% load increase

**Fig. 14.** Sensitivity analysis results on the Pareto frontier.

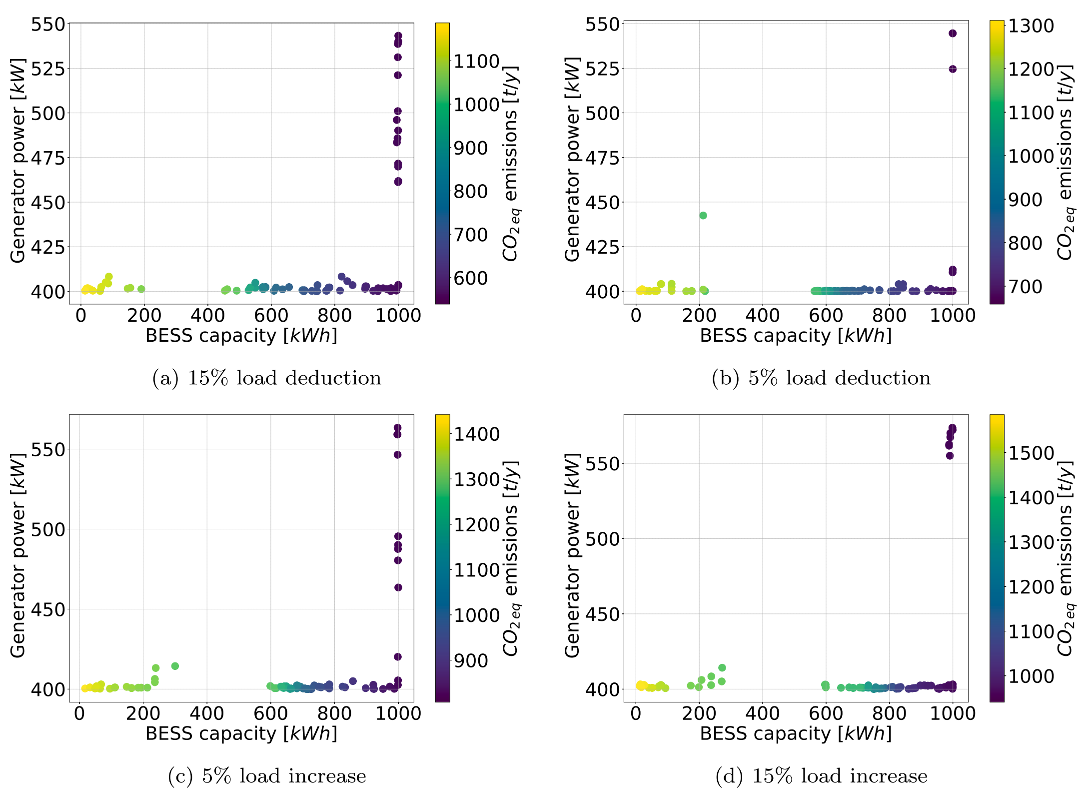


(a) 15% load deduction
(b) 5% load deduction
(c) 5% load increase
(d) 15% load increase

**Fig. 15.** Sensitivity analysis results on generated solutions.

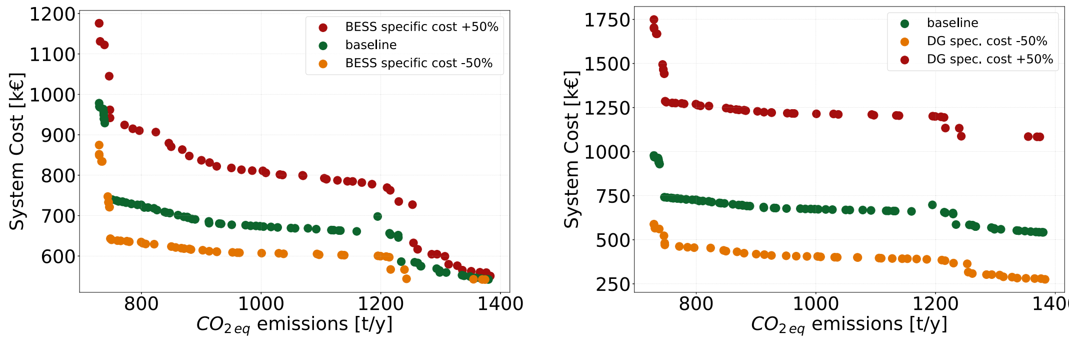


(a) BESS specific cost variation (b) DG specific cost variation

**Fig. 16.** Sensitivity of the Pareto frontier to variations in component specific cost.

## 6. Conclusion

This study proposed a nested optimization framework for marine hybrid propulsion systems. The proposed framework integrated power management optimization with optimal component sizing to capture the multidimensional nature of the design problem. The inner optimization layer focuses on minimizing greenhouse gas emissions by determining the optimal power split among available energy sources. The outer layer supports system sizing by identifying configurations that balance environmental performance with total system investment cost. This nested structure enables the identification of Pareto-optimal solutions, supporting design choices that balance emission-reduction goals with economic constraints.

To demonstrate the potential of the proposed methodology, a case study was analyzed and compared against a standard requirement-based design approach. The results highlight significant quantitative advantages, showing potential reductions of up to 27% in emissionsat the same investment cost, or a 6% cost saving at the same emission level relative to RBD baseline. These findings suggest that the integrated approach is a valuable decision-making tool for the preliminary design stages of low-emission vessels.

Furthermore, the presented approach was validated through a methodological benchmark and extensive sensitivity analyses. The accuracy of the optimization results was verified against an exhaustive grid search. This confirmed the NSGA-II algorithm's reliability in identifying the global Pareto frontier. Convergence was assessed by discussing the frontier behavior at different population sizes and generations. Robustness was evaluated by perturbing both the power demand profile and the component investment costs. The results demonstrate the stability and robustness of the proposed methodology, as well as its limited sensitivity to load fluctuations. These findings confirm that the developed optimization tool is not only reliable for the case study considered but also generalizable to different vessel types and mission profiles.

Several research directions can further improve the applicability and robustness of the proposed framework. Future developments should aim to validate and generalize the decision support tool, for example, by using randomized mission profiles based on the unit's annual operational profile. Extending the tool to include fuel cells powered by different hydrogen sources and generators that use alternative fuels, such as methanol, would further enhance its flexibility. As the maritime industry advances toward low- and zero-emission solutions, the combination of advanced optimization techniques with emerging propulsion technologies will be essential to achieving sustainable, economically viable outcomes. The methodologies presented in this paper provide a solid foundation for designing hybrid propulsion systems that meet regulatory requirements while enhancing environmental and economic performance.

## CRediT authorship contribution statement

**Luca Maloberti:** Writing – original draft, Visualization, Software, Methodology, Investigation, Formal analysis, Data curation, Conceptualization; **Raphael Zaccone:** Writing – review & editing, Validation, Supervision, Software, Methodology, Formal analysis, Conceptualization.

## Declaration of competing interest

The authors declare that they have no known competing financial interests or personal relationships that could have appeared to influence the work reported in this paper.

## References

Al-Falahi M.D., Nimma K.S., Jayasinghe S.D., Enshaei H., Guerrero J.M., 2018. Power management optimization of hybrid power systems in electric ferries, Energy Convers. Manage. 172 (2018) 50–66.
Ančić I., Vladimir N., Cho D.S., 2018. Determining environmental pollution from ships using index of energy efficiency and environmental eligibility (i4e), Mar. Policy 95 (2018) 1–7.
Ashok B., Nanthagopal K., Vignesh D.S., 2018. Calophyllum inophyllum methyl ester biodiesel blend as an alternate fuel for diesel engine applications, Alexandria Eng. J. 57 (2018) 1239–1247.
Basciu F., Casali G., Maloberti L., Pais T., Vergassola G., Zaccone R., 2025. Sustainable yacht refits: structural solutions in methanol-powered conversion, Ocean Eng. 323 (2025) 120618.
Belvisi D., Figari M., 2026. Multi-objective optimisation-based approach for shipboard energy-efficient battery energy storage sizing leveraging operational data, Appl. Energy 404 (2026) 126983.
Belvisi D., Maloberti L., Zaccone R., Figari M., 2024. Battery energy storage system sizing strategy for naval vessels through multi-objective optimisation, in: Conference Proceedings of iSCSS, 2024.
Bouman E.A., Lindstad E., Rialland A.I., Strømman A.H., 2017. State-of-the-art technologies, measures, and potential for reducing ghg emissions from shipping–a review, Transp. Res. Part D Transp. Environ. 52 (2017) 408–421.
Cabezas-Basurko O., Mesbahi E., Moloney S., 2008. Methodology for sustainability analysis of ships, Ships Offshore Struct. 3 (2008) 1–11.
Cha M., Enshaei H., Nguyen H., Jayasinghe S.G., 2024. Optimal sizing and evaluation of efficient fuel cell utilization for fuel cell battery hybrid electric ferry, Energy Convers. Manage. 315 (2024) 118723.
D'Agostino F., Gallo M., Saviozzi M., Silvestro F., 2023. A security-constrained optimal power management algorithm for shipboard microgrids with battery energy storage system, in: 2023 IEEE International Conference on Electrical Systems for Aircraft, Railway, Ship Propulsion and Road Vehicles & International Transportation Electrification Conference (ESARS-ITEC), IEEE, (2023), pp. 1–6.
Fruzzetti C., Donnarumma S., Maggiani F., Martelli M., 2024. Probabilistic operability and greenhouse gas assessment during dynamic positioning operations, Proc. Inst. Mech. Eng. Part M J. Eng. Marit. Environ. 238 (2024) 336–347.
Ghimire P., Zadeh M., Thorstensen J., Pedersen E., 2021. Data-driven efficiency modeling and analysis of all-electric ship powertrain: a comparison of power system architectures, IEEE Trans. Transp. Electrif. 8 (2021) 1930–1943.
IMO, 2018. 2018 initial IMO strategy. https://www.imo.org/en/OurWork/Environment/Pages/Vision-and-level-of-ambition-of-the-Initial-IMO-Strategy.aspx.
Inal O.B., Charpentier J.F., Deniz C., 2022. Hybrid power and propulsion systems for ships: current status and future challenges, Renew. Sustainable Energy Rev. 156 (2022) 111965.
Isotta Fraschini Motori, 2026. Isotta fraschini motori. https://www.isottafraschini.it/.

Jägerbrand A.K., Brutemark A., Sveden J.B., Gren M., 2019. A review on the environmental impacts of shipping on aquatic and nearshore ecosystems, Sci. Total Environ. 695 (2019) 133637.

Jimenez V.J., Kim H., Munim Z.H., 2022. A review of ship energy efficiency research and directions towards emission reduction in the maritime industry, J. Cleaner Prod. 366 (2022) 132888.

Kanellos F., 2013. Optimal power management with GHG emissions limitation in all-electric ship power systems comprising energy storage systems, IEEE Trans. Power Syst. 29 (2013) 330–339.

Lindstad E., Lagemann B., Rialland A., Gamlem G.M., Valland A., 2021. Reduction of maritime GHG emissions and the potential role of e-fuels, Transp. Res. Part D Transp. Environ. 101 (2021) 103075.

Maloberti L., 2025. Towards sustainable design of zero-emission ships, Ph.D. thesis. https://doi.org/10.15167/maloberti-luca_phd2025-05-09.

Maloberti L., Adami G., Figari M., Zaccone R., 2024. Evaluating alternative fuels and power systems for marine hybrid propulsion, in: Advances in Maritime Technology and Engineering: Volume 2 (2024) 45.

Maloberti L., Zaccone R., 2025. An environmentally sustainable energy management strategy for marine hybrid propulsion, Energy 316 (2025). https://doi.org/10.1016/j.energy.2025.134517.

Maloberti L., Zaccone R., Angius M., Martelli M., 2025a. A zero-emission propulsion system for a sustainable whale watching catamaran, Lect. Not. Netw. Syst. (2025). https://doi.org/10.1007/978-3-032-01620-1_22.

Maloberti L., Zaccone R., De Gaetano J., Campora U., 2025b. A comparison among innovative hybrid propulsion systems to reduce the environmental impact of a small passenger ship, Sustainable Energy Technol. Assess. 75 (2025) 104194.

Maloberti L., Zaccone R., Gualeni P., Mazzucchelli P., 2022. A zero-emission ferry for inland waterways, in: Technology and Science for the Ships of the Future, IOS Press, (2022), pp. 162–169.

Mueller N., Westerby M., Nieuwenhuijsen M., 2023. Health impact assessments of shipping and port-sourced air pollution on a global scale: a scoping literature review, Environ. Res. 216 (2023) 114460.

Tadros M., Ventura V., Soares C.G., 2023. Review of current regulations, available technologies, and future trends in the green shipping industry, Ocean Eng. 280 (2023) 114670.

UNFCCC, 2016. The Paris Agreement, United Nations Framework Convention on Climate Change. https://unfccc.int/sites/default/files/resource/parisagreement_publication.pdf.

Wang S., Psaraftis H.N., Qi J., 2021a. Paradox of international maritime organization's carbon intensity indicator, Commun. Transp. Res. 1 (2021) 100005.

Wang X., Shipurkar U., Haseltalab A., Polinder H., Claeys F., Negenborn R.R., 2021b. Sizing and control of a hybrid ship propulsion system using multi-objective double-layer optimization, IEEE Access 9 (2021) 72587–72601.

Wang X., Zhu H., Luo X., Chang S., Guan X., 2024. A novel optimal dispatch strategy for hybrid energy ship power system based on the improved NSGA-II algorithm, Electr. Power Syst. Res. 232 (2024) 110385.

Wu P., Bucknall R., 2020. Hybrid fuel cell and battery propulsion system modelling and multi-objective optimisation for a coastal ferry, Int. J. Hydrogen Energy 45 (2020) 3193–3208. https://doi.org/10.1016/j.ijhydene.2019.11.152.

Zaccone R., Campora U., Martelli M., 2021. Optimisation of a diesel-electric ship propulsion and power generation system using a genetic algorithm, J. Mar. Sci. Eng. 9 (2021) 587.

Zaccone R., Figari M., Martelli M., 2018. An optimization tool for ship route planning in real weather scenarios, in: ISOPE International Ocean and Polar Engineering Conference, ISOPE, (2018), pp. ISOPE–I.

Zhang Q., Xiong F., Zeng Y., Yu H., 2024. Collaborative optimization of zero-emission vessels considering power system volume and operation economy, Int. J. Hydrogen Energy 90 (2024) 1059–1069.